Late Season Imagery for Harvest Management

J.K. Ward, R.C. Phillips, G.T. Roberson

Biological and Agricultural Engineering, North Carolina State University, Raleigh, NC

A paper from the Proceedings of the
14th International Conference on Precision Agriculture
June 24 – June 27, 2018
Montreal, Quebec, Canada

Abstract. The overall objective of this project was to preliminarily assess the use of UAV-based thermal imagery to sense harvest-related factors. Results suggested that thermal imagery can be used to detect areas of high grain moisture content late in the harvest season. Time periods closer to physiological maturity were less likely to show significant differences in thermal imagery data. Additional research is needed to determine if moisture content trends with other measurable quantities such as vegetative indices or green color intensity.

Keywords. *thermal imagery, UAV, UAS, corn, harvest*

Introduction

Remote sensing in row-crop agriculture has emphasized early and mid-season data collection. Early season data largely focused on emergence, population, or stand. These data were typically collected using color imagery to detect green crop against bare soil background. Mid-season remote sensing has been used to monitor crop health, typically using vegetative indices such as NDVI or derivatives, to reflect crop stress from nutrient or moisture deficiency, disease, or other stressors. All of these data were used to manage crops or inputs to maximize productivity. Variation at harvest can still introduce issues that reduce total productivity by causing harvest losses or by reducing the value of the crop.

Ward et al. (2016) previously investigated variability in crop harvest moisture content across hybrids. There were significant differences of a magnitude which would impact harvest performance, yield data quality, and crop storability. Once these differences were measured, the next logical step was to identify methods to detect and manage them.

Thermal infrared imagery has been successfully used to measure canopy temperature from irrigation systems, manned aircraft, and unmanned aerial systems (UAS). Barnes et al. (2000) combined visible imagery, near infrared, and thermal infrared imagery on a lateral irrigator to assess nitrogen and water stress. Sullivan et al. (2007) assessed thermal imagery and found results to be stable over multiple flights and correlated imagery output to water stress comparing dryland and irrigated plots. Ford et al. (2017) used thermal imagery to differentiate areas of high and low irrigation rates.

No published work has been identified which related thermal imagery to crop status post physiological maturity.

Objectives

The objectives of this study were to: 1.) preliminarily access the use of UAV-based imagery to sense harvest-related factors, 2.) to identify variability in late-season thermal imagery, and 3.) use low-cost, off-the-shelf components.

Materials and Methods

Test plots were established at the R.R. Foil Plant Sciences Research Center on the campus of Mississippi State University near Starkville, Mississippi. A total of eighteen different corn (maize, *Zea mays*) hybrids were planted on 4 May, 2015 (Table 1). The hybrids were planted at a population of 74,074 seeds/ha (30,000 seeds/ac) on a 97 cm (38 in) row spacing. Each plot was 9.1 m (30 ft) long by four rows wide. The middle two rows were harvested for yield, not discussed in this analysis, and the exterior two rows were designated for sample collection, described below. All plots were placed on fine sandy loam of the same classification and received the same agronomic and pest management treatments. Moisture and heat units were non-limiting for this study.

Table 1. Study treatment numbers, hybrids, and relative maturities (RM)

ID	Source	RM
1	DKC 49-29	99
2	DKC 50-84	100
3	DKC 53-78	103
4	DKC 54-38	104
5	DKC 55-93	105
6	DKC 60-63	110
7	DKC 62-08	112
8	DKC 67-57	117
9	DKC 69-29	119
10	PHB 106	110
11	PHB 1197	111
12	PHB 1637	116
13	PHB 2089	120
14	2V717	111
15	2C799	113
16	2J794	115
17	AGR-N68	111
18	AGR-N79	115/116

Imagery Data

Thermal imagery was collected with a FLIR Tau 2 non-radiometric thermal camera. Non-radiometric imagery does not indicate the actual temperature of the target, but measures the relative differences in total emitted infrared radiation – which is correlated to temperature. Since the camera was dynamically scaled, all of the plots needed to be captured in the same image. All imagery was collected at US Federal Aviation Administration (FAA) mandated maximum altitude of 122 m (400 ft) above ground level (AGL). The resulting ground sampling distance (GSD) was 0.3 m (~12 in). During flights, video from the thermal camera was wirelessly transmitted to a computer at the ground control station. When all plots were in frame, an image was captured resulting in a geo-referenced gray-scale image in tagged image file (TIF) format. Only one capture was needed so no image stitching was required. All imagery and spatial data were handled using QGIS Desktop 3.0.0.

Immediately after planting, the corner location of each plot was captured with a survey-grade GNSS receiver. Polygons were created by joining the points located at plot corners. Plot polygons were buffered inward by 0.5 m to reduce the impact of edge effects on resulting data. The gray-scale thermal image and polygon layer were imported into QGIS then the Zonal Statistics Tool was used to extract and analyze pixels located within the plot polygon boundaries (Figure 1). Values collected from the raster layer include the number of pixels, mean eight-bit gray-scale value, standard deviation, maximum value, minimum value, and the range. Imagery returns range from 0 to 255 with 0 (black) being lower in temperature than 255 (white).

Imagery data was targeted for weekly collection starting at 100 days after planting (DAP), but weather and equipment failure prevented two flights (Table 2).

Figure 1. Thermal image GeoTiff raster overlaid with plot polygons.

Moisture Content Data

Grain wet-basis moisture content (MC) was determined for five selected treatments representing a range of relative maturity (RM). Ears were sampled at 102, 106, 109, 116, and 121 DAP (Table 2). Four ears were randomly selected from each plot, two from each outermost plot row. During the earliest sample dates, corn moisture content was high which prevented shelling without damaging the kernels. Ears were frozen to allow shelling and for consistency all sample dates were frozen prior to shelling. Shelled kernels were from all ears in a plot were comingled. Duplicate 100 g subsamples were weighed, dried for 24 hours at 103°C, and reweighed according to ASABE standard methods.

Table 2. Thermal imagery and moisture content data collection events. The (X) represents that data was collected while a (-) represents data was not collected.

Date	DAP	MC Data	Thermal Imagery
Aug 14 2015	102	X	-
Aug 18 2015	106	X	X
Aug 21 2015	109	X	X
Aug 28 2015	116	X	-
Sep 02 2015	121	X	X

Experimental Design and Analysis

The study was designed as a randomized complete block with four replications. All analyses were conducted using SAS 9.4. All three imagery data collection events were analyzed separately using a mixed effects model. MC data were analyzed using mixed effects with repeated measures. The subject was each plot nested into the replication. Significance and means separation was determined at 0.05 significance.

Results and Discussion

Thermal Imagery

Significant differences in thermal imagery returns were not present for the first flight at 106 DAP, but were identified for later flights at 109 and 121 DAP (Table 3). For all sample events, replicate effects and the interaction between replicates and treatment were insignificant. In this analysis, the numerical values of the mean eight-bit gray value are less meaningful than the relative comparison of their ranking within each sample event.

Table 3. Mean and standard error of eight-bit gray-scale thermal returns.

			106 DAP		109 DAP			121 DAP		
ID	Hybrid	RM	Mean	SE	Mean		SE	Mean		SE
1	DKC 49-29	99	121.8	25.3	88.3	a	10.3	125.7	a	18.1
2	DKC 50-84	100	127.5	9.2	87.5	a	8.5	127.2	a	6.21
3	DKC 53-78	103	113.6	7.9	78.5	abc	8.7	122.8	a	10.8
4	DKC 54-38	104	115.1	8.3	80.8	abc	5.1	103.6	abcd	6.8
5	DKC 55-93	105	124.3	17.6	84.0	ab	7.2	127.4	a	10.6
6	DKC 60-63	110	125.1	17.2	79.5	abc	4.6	96.8	abcd	15.1
7	DKC 62-08	112	103.3	21.4	71.5	abcd	7.6	113.5	ab	7.8
8	DKC 67-57	117	115.0	19.4	81.3	abc	9.0	111.3	ab	6.2
9	DKC 69-29	119	143.63	18.4	87.2	a	9.0	126.1	a	8.5
10	PHB 106	110	127.2	9.6	78.8	abc	4.8	106.1	abc	6.5
11	PHB 1197	111	140.6	17.9	61.1	cde	13.4	88.4	bcd	11.2
12	PHB 1637	116	95.3	27.3	51.7	de	4.0	74.3	d	10.2
13	PHB 2089	120	82.2	10.4	42.5	e	3.3	83.5	bcd	9.4
14	2V717	111	83.2	9.9	69.8	abcd	2.5	8575	bcd	12.5
15	2C799	113	132.6	7.1	51.9	de	6.9	76.4	cd	12.1
16	2J794	115	104.1	13.1	63.9	bcd	5.5	97.8	abcd	11.6
17	AGR-N68	111	97.8	5.8	77.4	abc	5.6	97.5	abcd	13.6
18	AGR-N79	115/116	91.6	5.7	72.0	abcd	4.5	88.5	bcd	14.0

Thermal imagery could be affected by wind or cloud cover but the result at 106 DAP could be a function of moisture stress early in physiological maturity before the onset of senescence. Note that DKC hybrids appear as a group to maintain higher temperatures than other hybrids. The lowest temperature for all sample dates occurs with a PHB hybrid with RM greater than 115 days. Further analysis of the impact of hybrid source, RM, and presence of specific genetic traits on late-season thermal imagery returns is needed. Additional consideration needs to be given to best normalization procedures to compare different sample periods to analyze trends over time.

Moisture Content

Grain MC was significantly different with respect to hybrid ($P < 0.0001$), DAP ($P < 0.0001$), and the interaction between hybrid and DAP ($P = 0.0016$) (Figure 2). These results were expected as different hybrids have been shown to field dry at different rates. The rates are not the same across time as weather and initial moisture content can affect the rate of moisture exchange between the kernel and the air. Finally, interaction significance was expected as hybrids respond to the environment differently.

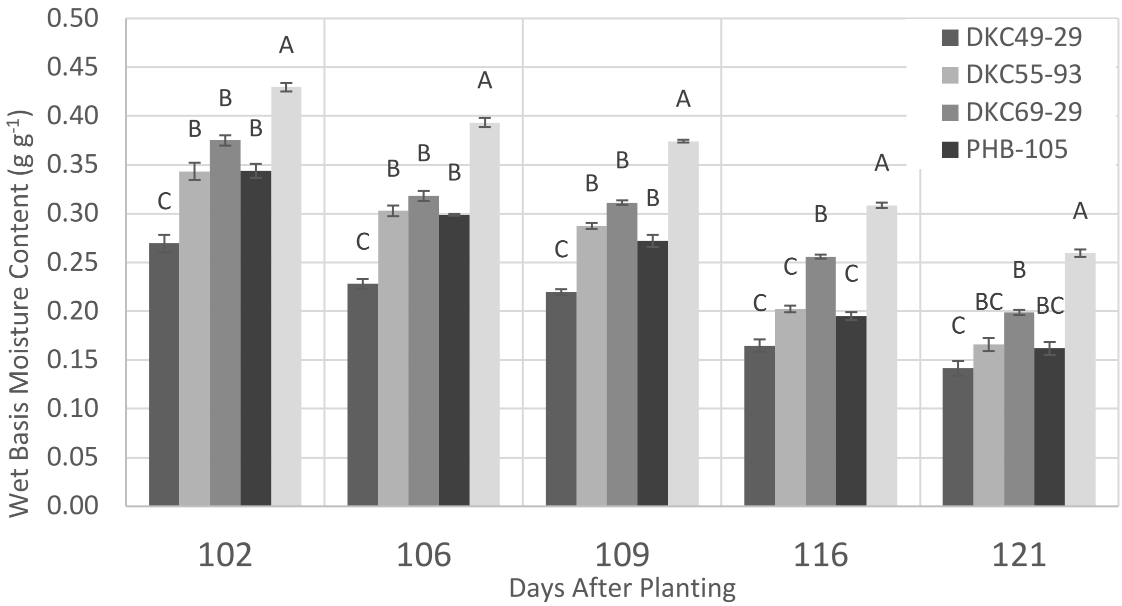

Figure 2. Mean grain wet-basis moisture content by days after planting. Means separated within each sample event.

Generally, hybrids maintained their relative rank of moisture contents. The hybrid with the maximum and minimum MC were the same for each DAP. The other three hybrid mean MCs were difficult to separate.

Relating Thermal Imagery with Moisture Content

There were significant differences in the mean digital thermal imagery values. There were also significant differences in grain MC. The key question is if these significant differences relate to one another. A subset of the digital thermal returns under analysis was created to coincide with the hybrids on which MC data were collected. At 106 DAP, there were not significant difference in thermal imagery, but there were significant differences in grain MC. Measured MC ranged from a high of 39% to a low of 23% with an indistinguishable mid-range of 30%-32% MC. At 109 DAP, there were significant differences in both MC and thermal values. The only different thermal value occurs with the hybrid with the greatest MC. AT 121 DAP, the results were similar. Significant differences among MC and thermal values were measured and there was greater stratification is the mean values. Again, the lowest thermal value coincides with the greatest MC.

Table 4. Mean grain wet-basis moisture content compared to digital thermal imagery returns. Means separated within each sample event.

DAP	Hybrid	Mean MC		SE	Mean Digital Value		SE
106	DKC4929	0.23	c	0.02	121.8	-	25.2
	DKC5593	0.30	b	0.02	124.3	-	17.6
	DKC6929	0.32	b	0.03	143.6	-	18.4
	PHB105	0.30	b	0.02	127.2	-	9.6
	PHB2089	0.39	a	0.01	83.2	-	10.4
109	DKC4929	0.22	c	0.01	88.3	a	10.3
	DKC5593	0.29	b	0.02	84.0	a	7.2
	DKC6929	0.31	b	0.03	87.2	a	9.0
	PHB105	0.27	b	0.02	78.8	a	4.8
	PHB2089	0.37	a	0.01	42.5	b	3.3
121	DKC4929	0.14	c	0.01	125.7	a	18.1
	DKC5593	0.17	bc	0.01	127.4	a	10.6
	DKC6929	0.20	b	0.01	126.1	a	8.5
	PHB105	0.16	bc	0.01	106.1	ab	6.5
	PHB2089	0.26	a	0.01	83.5	b	9.4

Summary

Results suggest that thermal imagery can be used to detect areas of high grain moisture content late in the harvest season. Time periods closer to physiological maturity were less likely to show significant differences in thermal imagery data. Using higher resolution imagery would likely improve results.

Additional research is needed to determine if moisture content trends with other measurable quantities such as vegetative indices or green color intensity.

Acknowledgements

Special thanks to Brien Henry, Louis Wasson, Christina Hall, and other who participated.

References

Barnes, E.M., Clarke, T.R., Richards, S.E., Colaizzi, P.D., Huberland, J., et al. (2000). Coincident detection of crop water stress, nitrogen status and canopy density using ground-based multispectral data. In Proceedings of the Fifth International Conference on Precision Agriculture (unpaginated cd-rom).

Ford, T., Hartman, C., Nagchaudhuri, A., Mitra, M., Marsh, L. (2017) Analysis of yield response with deficit drip irrigation strategies, remote sensing with UAVs, and thermal image processing. In 2017 ASABE Annual International Meeting. St. Joseph, MI.: ASABE.

Sullivan, D.G., Fulton, J.P., Shaw, J.N., Bland, G.L. (2007). Evaluating the sensitivity of an unmanned thermal infrared aerial system to detect water stress in a cotton canopy. Transaction of the ASABE, 50(6): 1963-1969.

Ward, J.K., Henry, W.B, Hock, W.M. (2017). Variability in harvest moisture and dry-down in multi-hybrid planting systems. Transactions of the ASABE, 59(5):1111-1115. St. Joseph Mich: ASABE.